CONDUCTION SHAPE FACTOR MODELS FOR 3-D ENCLOSURES

P. Teertstra[†], M. M. Yovanovich[‡] and J. R. Culham[⋆]
Microelectronics Heat Transfer Laboratory
Department of Mechanical Engineering
University of Waterloo
Waterloo, Ontario, Canada   N2L 3G1
http://www.mhtlab.uwaterloo.ca

Abstract

Analytical models are presented for conduction shape factors for three-dimensional regions formed between an isothermal, arbitrarily-shaped body and its concentric, arbitrarily-shaped surrounding enclosure. The model is based on the exact solution for the concentric spheres and two methods are developed to predict the effective gap spacing. The models are validated using existing numerical data from the literature and data from simulations performed using a commercial CFD software package. The models are shown to be in excellent agreement with the data for all enclosures with geometrically similar boundary shape, within 3% RMS. For enclosures formed between different boundary shapes, the models are shown to be accurate within 5% RMS when the minimum aspect ratio, i.e. the smallest outer boundary dimension over the largest inner dimension, is greater than 1.5.

Nomenclature

a, b, c	=	cuboid side dimensions, m
A	=	area, m^2
d	=	diameter, m
k	=	thermal conductivity, W/mK
L	=	general characteristic length, m
m	=	combination parameter
n	=	outward facing normal vector
Q	=	total heat flow rate, W
$\vec{r}$	=	general radial coordinate
R	=	thermal resistance, K/W
s	=	cube side length, m
S	=	conduction shape factor, m
$S_L^\star$	=	dimensionless conduction shape factor; $\equiv SL/A_i$
T	=	temperature, ${}^oC$
V	=	enclosed volume, m^3
x, y, z	=	Cartesian coordinates

Greek Symbols

δ	=	gap spacing; $\equiv (d_o - d_i)/2$, m
ϕ, θ	=	spherical coordinates
ψ	=	dimensionless temperature rise
ρ	=	local radial position, m

Subscripts

e	=	effective
i	=	inner
o	=	outer
∞	=	full-space limit

Introduction

Analytical models for conduction shape factors for three-dimensional regions formed between an arbitrarily-shaped, heated body and its surrounding, cooled enclosure are of some interest to thermal designers of sealed enclosures for microelectronics applications. Analytical heat transfer models can be used to quickly and accurately predict operating temperatures of circuit boards and components in the enclosure, providing a tool for parametric studies and trade-off analyses during the preliminary design process. An important step in the formulation of natural convection models for these applications is the development of conduction models in the enclosed region.

The problem of interest in the current study involves steady state conduction in the isotropic region bounded by concentric, arbitrarily-shaped isothermal boundaries, as shown in Fig. 1. Geometries examined include enclosed regions between similar body shapes with constant or near-constant gap thickness, as well as enclosures with different inner and outer boundary shapes.
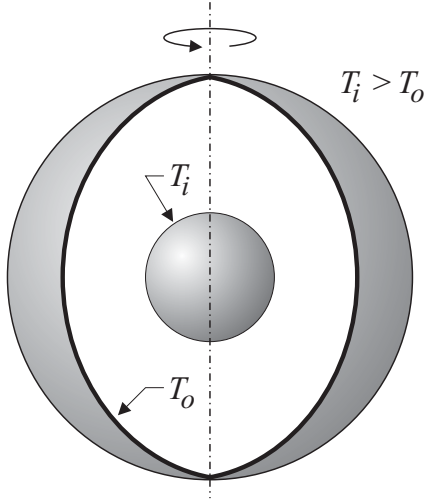
Fig. 1 Schematic of Physical Problem

Numerical data are available in the literature for steady state conduction for a limited set of enclosure geometries. Hassani[1] presents data for the concentric circular cylinders and the concentric base-attached cones for a wide range of gap spacing. Warrington et al.[2] presents numerical data for enclosures formed between different concentric boundary shapes for two cases: the cube in a spherical enclosure and the sphere in a cubical enclosure.

The only analytical model for the conduction shape factor in the literature is presented by Hassani and Hollands[3] for the dimensional shape factor S for 3-D enclosure geometries with uniform gap spacing:

$$S = (S_0^m + S_\infty^m)^{1/m} \qquad (1)$$

where S_∞ for the sphere is used to approximate all body shapes:

$$S_\infty = 3.51\sqrt{A_i}$$

and S_0 is approximated based on one-dimensional heat transfer:

$$S_0 = \frac{A_i}{\delta}$$

where δ is the minimum value of the gap spacing. The blended combination in Eq. (1) reduces to linear superposition, $m = 1$, for the concentric spheres. However, for boundary shapes where corners are present, such as the concentric cubes, a combination parameter value $m > 1$ is introduced. The values for m are dependent on geometry and are determined from a correlation of numerical data as a function of the inner body surface area, aspect ratio, and the enclosed volume. The model is restricted to enclosed regions formed between geometrically similar boundary shapes, such that the gap spacing is uniform. There are currently no analytical models available in the literature that address the problem of conduction for an enclosure with a non-uniform gap spacing.

The objective of the current study is to develop analytical models for the conduction shape factor for the general case of enclosures formed between two arbitrarily-shaped, isothermal boundaries. These models will be validated using the available numerical data from the literature, as well as data from a commercial CFD package for a variety of different boundary shapes.

Problem Definition

The conduction shape factor S is defined by Yovanovich[4] for an isolated, 3-D body shape based on an area integral of the temperature gradient along an outward facing normal n from the body surface:

$$S = \iint_{A_i} -\left.\frac{\partial \psi}{\partial n}\right|_{A_i} dA_i \qquad (2)$$

For the particular problem of the 3-D enclosure formed between a heated inner and cooled outer boundary, the integral is evaluated at the inner surface, A_i, where the dimensionless temperature rise ψ is defined as:

$$\psi = \frac{T(\vec{r}) - T_o}{T_i - T_o} \qquad (3)$$

The shape factor is non-dimensionalized using the general scale length L as follows:

$$S_L^\star = \frac{SL}{A_i} = \frac{L}{A_i} \iint_{A_i} -\left.\frac{\partial \psi}{\partial n}\right|_{A_i} dA_i \qquad (4)$$

The dimensionless shape factor is related to the thermal resistance R and total heat transfer rate Q by:

$$S_L^\star = \frac{L}{kA_i R} = \frac{QL}{kA_i(T_i - T_o)} \qquad (5)$$

The square root of the inner body surface area is selected as the characteristic length, $L = \sqrt{A_i}$, such that:

$$S_{\sqrt{A_i}}^\star = \frac{1}{k\sqrt{A_i}R} = \frac{Q}{k\sqrt{A_i}(T_i - T_o)} \qquad (6)$$

Figure 2 presents the range of different inner body shapes examined in this work, and shows the notation used to describe each of the dimensions. Similar notation is used for the dimensions of the outer boundary shapes.

Model Development

The concentric spherical enclosure is a fundamental case of the three-dimensional enclosures, where the thermal resistance can be determined using the expression presented in most heat transfer texts[5]:

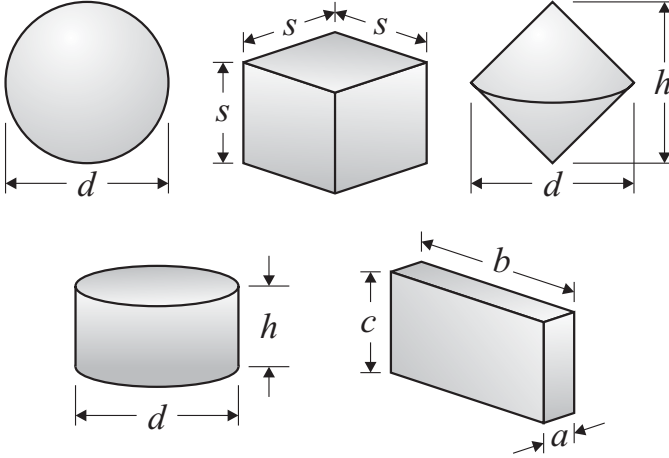$$R = \frac{1}{2\pi k}\left(\frac{1}{d_i} - \frac{1}{d_o}\right) \qquad (7)$$

2

Fig. 2 Inner and Outer Boundary Shapes

Using Eq. (6) to relate the resistance to the dimensionless conduction shape factor gives:

$$S^\star_{\sqrt{A_i}} = \frac{1}{k\sqrt{A_i}\,R} = \frac{2\sqrt{\pi}}{\left(1 - \dfrac{d_i}{d_o}\right)} \qquad (8)$$

However, the asymptotic characteristics of the shape factor solution for small and large values of aspect ratio, d_i/d_o, can be demonstrated more effectively by introducing the gap thickness, δ, defined as:

$$\delta = \frac{d_o - d_i}{2} \qquad (9)$$

Substituting $d_o = d_i + 2\delta$ into the expression for thermal resistance gives:

$$R = \frac{\delta}{\pi k d_i (d_i + 2\delta)} \qquad (10)$$

The corresponding dimensionless shape factor expression is:

$$\begin{aligned} S^\star_{\sqrt{A_i}} &= \frac{1}{k\sqrt{A_i}\,R} = \frac{1}{k\sqrt{\pi}\,d_i} \cdot \frac{\pi k d_i (d_i + 2\delta)}{\delta} \\ &= \frac{\sqrt{\pi}\,d_i}{\delta} + 2\sqrt{\pi} \end{aligned} \qquad (11)$$

This formulation for $S^\star_{\sqrt{A_i}}$ is a linear superposition of two limiting cases. For small values of gap spacing with respect to the inner body diameter, δ/d_i, the first term in Eq. (11) is dominant, corresponding to 1-D, planar resistance. For δ/d_i large, $S^\star_{\sqrt{A_i}}$ tends to a constant value corresponding to the dimensionless conduction shape factor for a sphere in a full-space region.
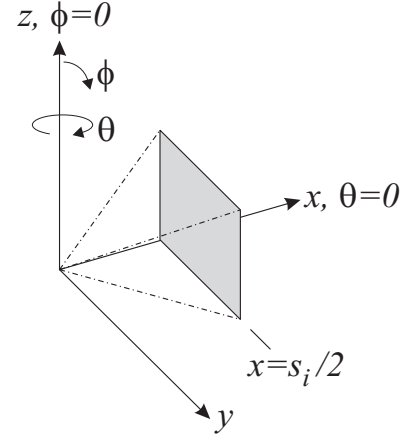

Fig. 3 Cube Surface Definition in Spherical Coordinates

Noting that the numerator of the first term in Eq. (11) corresponds to $\sqrt{A_i}$ for the sphere, a general model for dimensionless conduction shape factor for three-dimensional enclosures is proposed based on the exact solution for the concentric spheres:

$$S^\star_{\sqrt{A_i}} = \frac{\sqrt{A_i}}{\delta_e} + S^\star_{\infty} \qquad (12)$$

where $S^\star_{\infty}$ is the conduction shape factor for the inner body in a full space region. Models, tabulated values and correlations for $S^\star_{\infty}$ are available for a variety of body shapes in technical publications or handbooks.[4]

Effective Gap Spacing   The effective gap spacing in Eq. (12), δ_e, is an exact value in the case of enclosures with uniform gap thickness, such as the concentric spheres. However, for enclosures with different inner and outer boundary shapes or boundaries with sharp corners, approximate models are required to predict δ_e. In the proposed research study, two different models for the effective gap spacing are developed.

For certain geometries, it is possible to calculate the local gap thickness as a function of the angular position in spherical coordinates, where the origin is concentric with the inner and outer boundaries. For the particular example of a cube in a spherical enclosure, local gap thickness $\delta(\phi, \theta)$ is determined by:

$$\delta(\phi, \theta) = \frac{d_o}{2} - \rho_i(\phi, \theta) \qquad (13)$$

where $\rho_i(\phi, \theta)$ maps one quarter of the $x = s_i/2$ face of the cube in spherical coordinates, as shown in Fig. 3:

$$\rho_i(\phi, \theta) = \frac{(s_i/2)}{\sin\phi\cos\theta} \qquad (14)$$

$$0 \leq \theta \leq \pi/4, \qquad \tan^{-1}\sec\theta \leq \phi \leq \pi/2$$

3

The mean value for the effective gap spacing is determined by an area integration in spherical coordinates over the outer boundary, A_o:

$$\delta_e = \frac{24}{\pi d_o^2} \int_0^{\pi/4} \int_{\tan^{-1}\sec\theta}^{\pi/2} \delta(\phi,\theta) \frac{d_o^2}{4} \sin\phi\, d\phi\, d\theta \quad (15)$$

The integral is solved numerically to determine δ_e for different combinations of d_o and s_i.

For certain combinations of boundary shapes it may be difficult to define the local gap thickness as a mathematical function that can be integrated in the manner described. In this case, an alternate approximate modelling technique, called the *two-rule* method, can be used. In this method, the effective gap spacing is determined from the equivalent spherical enclosure in which the surface area of the inner boundary and the volume of the enclosed region are preserved. The diameter of the equivalent inner sphere is found by:

$$d_i = \sqrt{A_i/\pi} \quad (16)$$

The diameter of the equivalent outer spherical boundary is related to the volume of the inner body, V_i and the total enclosed volume, V, by:

$$d_o = \left[6\left(V + V_i\right)/\pi\right]^{1/3} \quad (17)$$

The volume of the inner sphere is related to its area by:

$$V_i = \frac{\pi}{6} d_i^3 = \frac{A_i^{3/2}}{6\sqrt{\pi}} \quad (18)$$

The effective gap spacing is determined by:

$$\begin{aligned}
\delta_e &= \frac{d_o - d_i}{2} = \frac{1}{2}\left[\left(\frac{6V}{\pi} + \frac{A_i^{3/2}}{\pi^{3/2}}\right)^{1/3} - \left(\frac{A_i}{\pi}\right)^{1/2}\right] \\
&= \frac{\sqrt{A_i}}{2\sqrt{\pi}}\left[\left(6\sqrt{\pi}\frac{V}{A_i^{3/2}} + 1\right)^{1/3} - 1\right] \quad (19)
\end{aligned}$$

Conduction Shape Factor   Given these two methods for calculating the effective gap spacing, the conduction shape factor can be determined based on Eq. (12). For the integral method, the conduction shape factor is:

$$S^\star_{\sqrt{A_i}} = \frac{\sqrt{A_i}}{\delta_e} + S^\star_\infty \quad (20)$$

where δ_e is determined based on a numerical solution to the integral, where necessary. In the case of the two-rule model, δ_e from Eq. (19) can be substituted into Eq. (12) to yield:

$$S^\star_{\sqrt{A_i}} = \frac{2\sqrt{\pi}}{\left[1 + 6\sqrt{\pi}\left(\frac{V^{1/3}}{\sqrt{A_i}}\right)^3\right]^{1/3} - 1} + S^\star_\infty \quad (21)$$

where the dimensionless independent parameter $V^{1/3}/\sqrt{A_i}$ is selected to match the order of the terms appearing in the general model, Eq. (12).

Model Application and Validation

In order to validate the conduction shape factor models for a variety of inner and outer boundary configurations, the following test cases are presented.

Geometrically-Similar Boundary Shapes Three different configurations of enclosures with geometrically similar boundaries are examined: concentric cubes; concentric circular cylinders; and concentric base-attached double cones. For each configuration, the ratio of the inner to outer boundary dimensions are varied such that the range of the independent parameter is:

$$0.2 \le \frac{V^{1/3}}{\sqrt{A_i}} \le 5$$

The conduction shape factor, $S^\star_{\sqrt{A_i}}$ is determined using the two-rule model, Eq. (21), as a function of the boundary dimensions defined in Fig. 2.

Concentric Cubes

$$V = s_o^3 - s_i^3 \ , \quad A_i = 6s_i^2$$

$$S^\star_{\sqrt{A_i}} = \frac{2\sqrt{\pi}}{\left(1 + \frac{\sqrt{\pi}}{6}\left[\left(\frac{s_o}{s_i}\right)^3 - 1\right]\right)^{1/3} - 1} + S^\star_\infty \quad (22)$$

where the conduction shape factor for the isolated cube in a full space domain is[4]

$$S^\star_\infty = 3.391$$

Concentric Circular Cylinders $(h/d = 1)$

$$V = \frac{\pi}{4}\left(d_o^2 h_o - d_i^2 h_i\right) \ , \quad A_i = 2\left(\frac{\pi}{4}d_i^2\right) + \pi d_i h_i$$

$$S^\star_{\sqrt{A_i}} = \frac{2\sqrt{\pi}}{\left(1 + \frac{2}{\sqrt{6}}\left[\left(\frac{d_o}{d_i}\right)^3 - 1\right]\right)^{1/3} - 1} + S^\star_\infty \quad (23)$$

where $S^\star_\infty$ is calculated by[4]

$$S^\star_\infty = \frac{3.1915 + 2.7726\left(\frac{h_i}{d_i}\right)^{0.76}}{\sqrt{1 + 2h_i/d_i}} = 3.443 \quad (24)$$
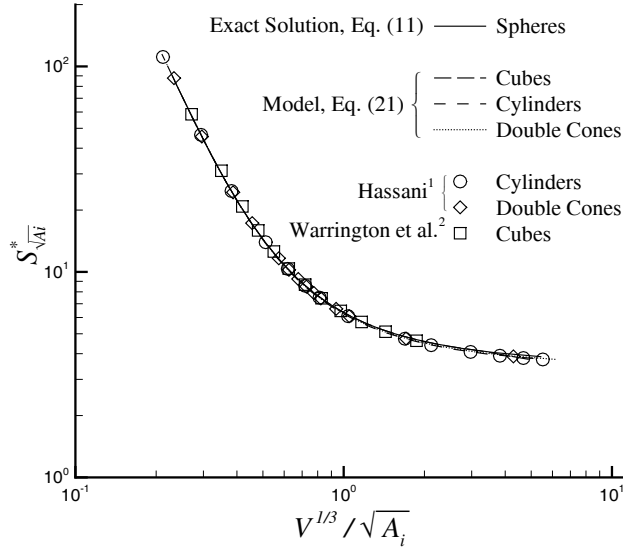
4

Fig. 4 Geometrically-Similar Boundary Shapes

Concentric Base-Attached, Double Cones $(h/d = 1)$

$$V = \frac{\pi}{12}\left(d_o^2 h_o - d_i^2 h_i\right) , \quad A_i = 2\left(\frac{\pi}{4} d_i h_i\right)$$

$$S^\star_{\sqrt{A_i}} = \frac{2\sqrt{\pi}}{\left(1 + \sqrt{2}\left[\left(\frac{d_o}{d_i}\right)^3 - 1\right]\right)^{1/3} - 1} + S^\star_\infty \quad (25)$$

where $S^\star_\infty$ is determined from the correlation[4]

$$\begin{aligned}S^\star_\infty &= 3.1943 + 0.6266\frac{h_i}{d_i} - 0.4778\left(\frac{h_i}{d_i}\right)^2 + \\ &\quad 0.0751\left(\frac{h_i}{d_i}\right)^3 + 0.0532\left(\frac{h_i}{d_i}\right)^4 = 3.471\end{aligned}$$

In Fig. 4 the model predictions for each of these enclosure configurations are compared with numerical data from Hassani[1] for the cylinders and base-attached double cones and from Warrington et al.[2] for the concentric cubes, as well as the exact solution for the concentric spheres. Figure 4 demonstrates the excellent agreement between the two-rule model and the data, with an RMS difference of 2.8% for the concentric cubes, and a difference of less than 1% RMS for both the cylinders and double cones. The use of $V^{1/3}/\sqrt{A_i}$ as the independent parameter and the square root of the inner body surface area as the scale length has effectively collapsed all the data and models to a single curve.

Cube in Spherical Enclosure The conduction shape factor for the region formed between a cube and a concentric, spherical enclosure is modelled using both the two-rule and integral methods. The ratio of the inner to the outer boundary dimensions are varied over a range corresponding to the available data from Warrington et al.[2]

$$0.5 \leq \frac{V^{1/3}}{\sqrt{A_i}} \leq 2$$

Using the two-rule model, the effective gap spacing, δ_e and the dimensionless conduction shape factor, $S^\star_{\sqrt{A_i}}$, are determined using Eqs. (19) and (20):

$$V = \frac{\pi}{6} d_o^3 - s_i^3 , \quad A_i = 6 s_i^2$$

$$\delta_e = \frac{s_i}{2}\left(\left[\left(\frac{d_o}{s_i}\right)^3 + \frac{6\left(\sqrt{6} - \sqrt{\pi}\right)}{\pi\sqrt{\pi}}\right]^{1/3} - \sqrt{\frac{6}{\pi}}\right) \quad (26)$$

$$S^\star_{\sqrt{A_i}} = \frac{2\sqrt{\pi}}{\left(1 + \frac{\pi\sqrt{\pi}}{6\sqrt{6}}\left[\left(\frac{d_o}{s_i}\right)^3 - \frac{6}{\pi}\right]\right)^{1/3} - 1} + 3.391$$
$$(27)$$

Since the geometry of both the spherical and cubical boundaries can be expressed in spherical coordinates, the integral method can also be used in this case. As described by Eqs. (13) and (14), the local gap thickness can be determined as a function of angular position, and the effective gap spacing is determined from an area average over the outer, spherical boundary. The integral shown in Eq. (15) can be partially evaluated to the following expression:

$$\begin{aligned}\delta_e &= \frac{s_i}{2}\left[\frac{d_o}{s_i} - 3\ln\left(1 + \sqrt{2}\right)\right] \\ &\quad + \frac{3 s_i}{\pi}\int_0^{\pi/4}\frac{\tan^{-1}\sec\theta}{\cos\theta}d\theta\end{aligned} \quad (28)$$

which can be evaluated numerically to give:

$$\delta_e = s_i\left[\frac{1}{2}\frac{d_o}{s_i} - 0.6107\right] \quad (29)$$

The conduction shape factor for the integral method is determined by substituting Eq. (29) into the general model for $S^\star_{\sqrt{A_i}}$, Eq. (20).

Figure 5 compares the predictions of the integral and two-rule models with numerical data from Warrington et al.[2]. The ratio of the diameter of the spherical enclosure and the cube side length, d_o/s_i, is also plotted versus $V^{1/3}/\sqrt{A_i}$ on the second y-axis. There is good agreement between both models and the data; however, the integral model provides a better fit of the data than the two rule model, within 3% RMS difference over the full range of the dimensionless gap spacing.
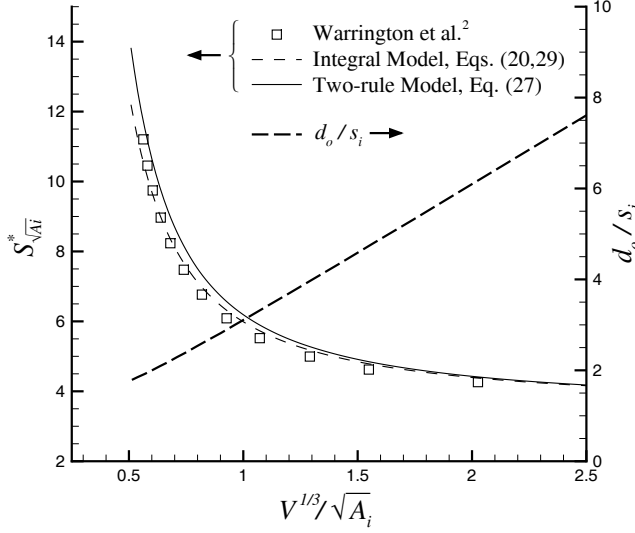
5

Fig. 5 Cube in Spherical Enclosure

Fig. 6 Sphere in Cubical Enclosure

Sphere in Cubical Enclosure For the sphere contained with a concentric cubical enclosure, both the two-rule and integral methods for predicting δ_e and $S^\star_{\sqrt{A_i}}$ are compared with the existing numerical data. Applying the two-rule model to this case gives the following:

$$V = s_o^3 - \frac{\pi}{6} d_i^3 \ , \quad A_i = \pi d_i^2$$

$$\delta_e = \frac{d_i}{2} \left[\left(\frac{6}{\pi} \right)^{1/3} \frac{s_o}{d_i} - 1 \right] \tag{30}$$

$$S^\star_{\sqrt{A_i}} = \frac{2\sqrt{\pi}}{\left[\left(\frac{6}{\pi} \right)^{1/3} \frac{s_o}{d_i} - 1 \right]} + 2\sqrt{\pi} \tag{31}$$

For the integral method analysis, the effective gap spacing is determined based on an area average on the inner spherical surface by interchanging d_o with d_i in Eq. (15), where $\delta(\phi, \theta)$ is

$$\delta(\phi, \theta) = \frac{(s_o/2)}{\sin\phi\cos\theta} - \frac{d_i}{2} \tag{32}$$

$$0 \leq \theta \leq \pi/4 \ , \quad \tan^{-1}\sec\theta \leq \phi \leq \pi/2$$

Partial evaluation of the integral gives:

$$\delta_e = \frac{3s_o}{2} \ln\left(1 + \sqrt{2}\right) - \frac{3s_o}{\pi} \int_0^{\pi/4} \frac{\tan^{-1}\sec\theta}{\cos\theta} d\theta - \frac{d_i}{2} \tag{33}$$

Evaluating the integral numerically yields:

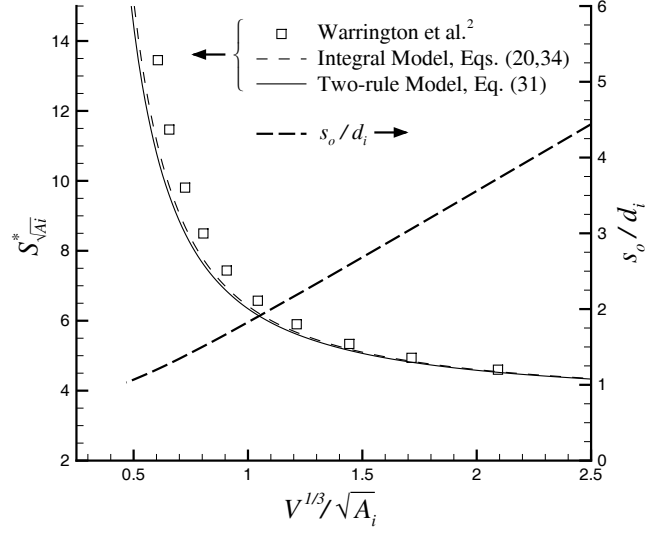$$\delta_e = d_i \left[0.6107 \frac{s_o}{d_i} - \frac{1}{2} \right] \tag{34}$$

Figure 6 compares the $S^\star_{\sqrt{A_i}}$ data of Warrington et al.[2] with both the two-rule and integral models, as well as the ratio s_o/d_i, as a function of $V^{1/3}/\sqrt{A_i}$. The agreement between the models and data is not as good as for the cube in a spherical enclosure; however, for $V^{1/3}\sqrt{A_i} > 1$, corresponding to $s_o/d_i > 2$, the RMS difference between both models and the data is less than 5%. The error becomes more significant for smaller gap spacing, where the diameter of the inner sphere approaches that of the outer boundary, leading to a local increase in heat transfer that is not accounted for in the model.

Cuboid in Cubical Enclosure In the next test case, the conduction shape factor for a cuboid with dimensions $(a, b = 3.785a, c = 2.175a)$ in a concentric cubical enclosure is modelled. Due to the complexity of formulating the limits on the integration for each of the faces of the cuboid, the integral method will not be used in this example. The two-rule model is applied as follows:

$$V = s_o^3 - abc \ , \quad A_i = 2ab + 2ac + 2bc$$

$$\frac{V^{1/3}}{\sqrt{A_i}} = \frac{\left(\frac{s_o^3}{abc} - 1 \right)^{1/3}}{\sqrt{2 (abc)^{1/3} \left(\frac{1}{a} + \frac{1}{b} + \frac{1}{c} \right)}} \tag{35}$$

$S^\star_{\sqrt{A_i}}$ is calculated using Eq. (20), where $S^\star_\infty$ is calculated using the model presented by Yovanovich[4] and Culham et al.[6] for the cuboid, which gives $S^\star_\infty = 3.469$.

The model is compared to numerical data from simulations performed using FLOTHERM[7], a commercial finite volume-based CFD package. Full details of the numerical procedure, including a grid convergence study,
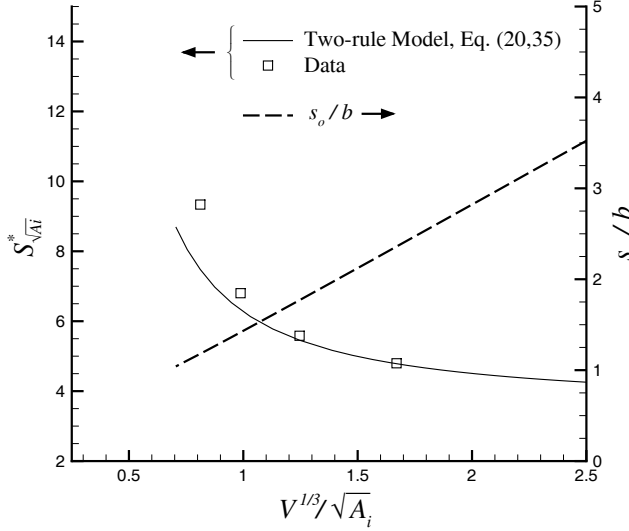
6

Fig. 7 Cuboid in Cubical Enclosure

Fig. 8 Cylinder in Cubical Enclosure

as given in the Appendix. The predictions of the two-rule model are compared with the numerical data in Fig. 7. As in the previous case, there is good agreement between the model and the data for values of $V^{1/3}/\sqrt{A_i} > 1$, corresponding to $s_o/b > 1.5$, with an RMS difference of less than 3%. More significant error occurs when $V^{1/3}/\sqrt{A_i} < 1$, where the longest dimension of the cuboid approaches the side length of the enclosure, $s_o/b < 1.4$. The local increase in the heat transfer caused by the close proximity of these surfaces is not accounted for in the model.

Cylinder in Cubical Enclosure The final test case involves a circular cylinder, $h_i/d_i = 0.5$, in a cubical enclosure. The two rule model formulation for $S^\star_{\sqrt{A_i}}$ is developed as follows:

$$V = s_o^3 - \frac{\pi}{4} d_i^2 h_i , \quad A_i = 2\left(\frac{\pi}{4} d_i^2\right) + \pi d_i h_i$$

$$\frac{V^{1/3}}{\sqrt{A_i}} = \sqrt{\frac{2}{\pi}} \frac{\left[\left(\frac{s_o}{d_o}\right)^3 - \frac{\pi}{4}\frac{h_i}{d_i}\right]^{1/3}}{\sqrt{2\,h_i/d_i + 1}} \tag{36}$$

Equation (20) is used to determine $S^\star_{\sqrt{A_i}}$, where $S^\star_\infty$ is calculated for $h_i/d_i = 0.5$ using Eq. (24).

The model predictions are validated using numerical results from simulations performed using FLOTHERM, as described in the Appendix. Figure 8 demonstrates the good agreement between the model and the data, within 2% RMS for $V^{1/3}/\sqrt{A_i} > 0.8$, corresponding to $s_o/d_i > 1.5$. The maximum difference of 10% occurred when the diameter of the cylinder approaches the dimensions of the enclosure, $s_o/d_i = 1.3$.
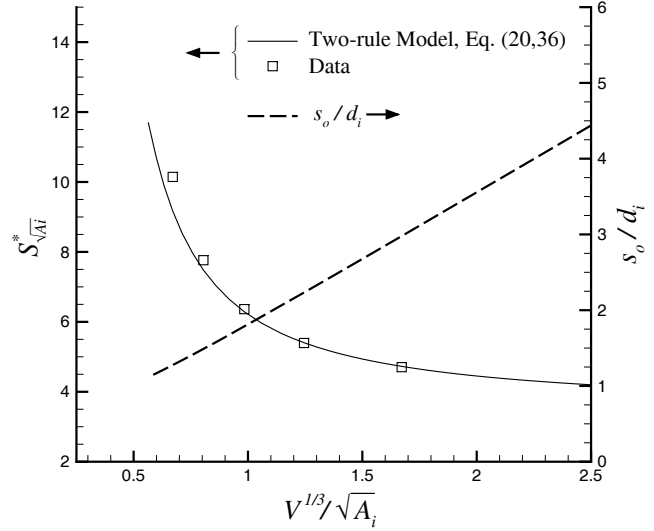
Summary and Conclusions

A general model has been presented for conduction shape factors between an arbitrarily-shaped, isothermal inner body and its surrounding, isothermal enclosure based on the exact solution for the concentric spheres. The model requires an effective value of the gap spacing and two approaches for determining δ_e, the integral method and the two-rule method, have been developed. The integral method provides better agreement than the two-rule method with the available numerical data; however, its use is limited to geometries where the local gap thickness and integration limits can be expressed mathematically. The two-rule method is a general model, applicable in all cases where the enclosed volume and inner body surface area can be determined.

The agreement between the two-rule model and the numerical data is excellent for all enclosures with geometrically similar boundary shapes, within 1 - 3 % RMS difference in all cases examined in this work. The two rule model is also effective in accurately predicting $S^\star_{\sqrt{A_i}}$ for enclosures with different inner and outer boundary shapes, with an RMS difference of 3 - 5 % in all cases when $V^{1/3}/\sqrt{A_i} > 1$. The model is less accurate for certain geometries, such as the sphere in a cubical enclosure, and the ratio of the smallest outer body dimension to the largest inner body dimensions, i.e. s_o/d_i, can be used to indicate the range of application of the model. In all cases, the accuracy of the two-rule model is significantly reduced when the corresponding ratio of outer and inner dimensions is less than 1.5. In these situations, numerical simulation may be required in order to accurately determine the conduction shape factor.

7

Acknowledgments

References

[1] Hassani, A.V., "An Investigation of Free Convective Heat Transfer from Bodies of Arbitrary Shape," Ph.D. Thesis, Department of Mechanical Engineering, University of Waterloo, Waterloo, Ontario, Canada, 1987.

[2] Warrington, R.O., Powe, R.E. and Mussulman, R.L., "Steady Conduction in Three-Dimensional Shell," *Journal of Heat Transfer,* Vol. 104, pp. 393 - 394, 1982.

[3] Hassani, A.V. and Hollands, K.G.T., "Conduction Shape Factor for a Region of Uniform Thickness Surrounding a Three Dimensional Body of Arbitrary Shape," *Journal of Heat Transfer,* Vol. 112, pp. 492 - 495, 1990.

[4] Yovanovich, M.M., "Conduction and Thermal Contact Resistances (Conductances)," *Handbook of Heat Transfer,* 3rd. ed., eds. W.M. Rohsenow, J.P. Hartnett and Y. Cho, McGraw Hill, New York, Chapter 3, pp. 3.1 - 3.73, 1998.

[5] Incropera, F.P. and DeWitt, D.P., *Fundamentals of Heat and Mass Transfer,* 4th ed., Wiley, New York, pp. 96 - 99, 1996.

[6] Culham, J.R., Yovanovich, M.M., Teertstra,P., Wang, C.-S., Refai-Ahmed, G. and Tain, R., "Simplified Analytical Models for Forced Convection Heat Transfer from Cuboids of Arbitrary Shape," *Journal of Electronic Packaging,* Vol. 123, No. 3, pp. 182 - 188, 2001.

[7] FLOTHERM, Flomerics Inc., Southboro, MA, 01772, 2002.

Appendix

All numerical data for the cuboid-in-cube and cylinder-in-cube enclosures were calculated using FLOTHERM[7], a commercial finite volume based CFD software package. The CFD modelling is performed in a three-dimensional domain, and the mode of heat transfer is limited to conduction only. The software uses an orthogonal grid in Cartesian coordinates and is well suited to problems involving cubes and cuboids; however, FLOTHERM also includes angled plates that are used to create complex objects, such as the circular cylinder.

The models for the cuboid and the cylinder are simplified by assuming 1/8 symmetry, with adiabatic boundary conditions imposed at all symmetry ($x = 0, y = 0, z = 0$) boundaries and isothermal boundary conditions at all outer boundaries, $T_o = 25^oC$. The surface of the inner body is treated as an isothermal boundary condition,
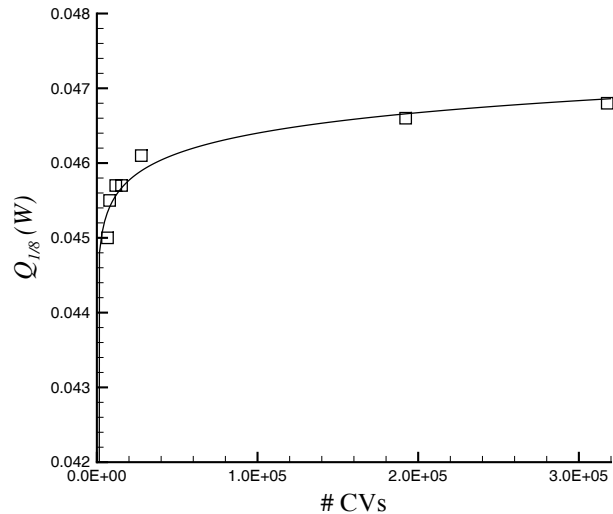

Fig. 9 Grid Convergence Results for Cylinder in Cubical Enclosure

$T_i = 50^oC$. In order to vary the aspect ratio of the enclosure, the inner boundary dimensions are changed while the outer boundary was held constant. A constant value for the thermal conductivity, $k = 0.0261 W/mK$, is specified for the region between the source and the outer boundary. The software automatically calculates the total heat flow rate crossing the inner boundary based on an area-weighted sum of the fluxes calculated from the local temperature gradient.

Grid independence was verified for the cylinder-in-cube configuration for the following test case:

$$
\begin{aligned}
d_i &= 60\, mm \\
h_i &= 30\, mm \\
s_o &= 134\, mm
\end{aligned}
$$

The total heat transfer rate is plotted as a function of the number of control volumes in Fig. 9.

The grid convergence study demonstrates that the use of approximately 200,000 control volumes for the simulation results in a solution for Q that is independent of the number of grid points. All subsequent numerical simulations were performed using the same level of mesh refinement.

The results of the FLOTHERM simulations are expressed in terms of the total heat transfer rate for the 1/8 symmetry problem, $Q_{1/8}$. In order to compare these data with the model predictions, the following non-dimensionalization is performed:

$$
S^\star_{\sqrt{A_i}} = \frac{8\left(Q_{1/8}\right)}{k\sqrt{A_i}\Delta T}
$$

where values of k and $\Delta T = T_i - T_o$ are given above and $\sqrt{A_i}$ is the square root of the total inner boundary surface area.

8